Theor Chem Acc (2004) 111:287–302
DOI 10.1007/s00214-003-0538-z

Theoretical
Chemistry Accounts

Regular article

Theoretical investigation on the oxazaborolidine-ketone interaction in small model systems

Giuliano Alagona[1], **Caterina Ghio**[1], **Simone Tomasi**[2]

[1] CNR-IPCF, Molecular Modeling Lab., Istituto per i Processi Chimico-Fisici, Via Moruzzi 1, 56124, Pisa, Italy
[2] Dipartimento di Chimica e Chimica Industriale, Via Risorgimento 35, 56126, Pisa, Italy

Received: 15 January 2003 / Accepted: 30 April 2003 / Published online: 23 January 2004

Abstract. The reduction of ketones by borane (BH_3) using the Corey, Bakshi and Shibata (CBS) catalyst is an important tool in asymmetric synthesis. In a theoretical study of the reduction of acetophenone, substantial differences emerged depending on the method and basis set adopted. Therefore, in this work, the weak interaction responsible for the formation of the acetophenone-CBS complex was studied for model systems, with the aim to find the best compromise between the quality of the interaction description achieved and computational costs. The main model chosen for the study contained the most important elements of the acetophenone-CBS-BH_3 complexes: the 1,3,2-oxazaborolidine ring, with molecules of BH_3 and acetone (the smallest possible ketone) coordinated to it. The effect of basis set and method on the description of the ketone-oxazaborolidine interaction along the B···O approach path was investigated via several methods (HF, DFT-B3LYP, MP2) and basis sets (3–21G, 6–31G, 6–31G*, 6–31G**, 6–31 + G**), taking into account basis set superposition errors, which can be significant even in the case of interactions involving two relatively large systems. Due to the remarkable structural changes occurring in the process, the effects of geometry deformation were also considered. The complexation of acetone is largely due to the electrostatic interaction between a Lewis acid/base couple: the endocyclic boron and the carbonyl oxygen respectively. The electron density drawn away from the C = O double bond makes the carbon atom more susceptible to hydride transfer, while the presence of the ring keeps the system rigid. The MP2 results turn out to be the closest to the QCISD(T) results from QCISD(T)/6–31G*//HF/6–31G* calculations. In order to improve the analysis of the nature of the interactions taking place in the complex, several dimers, smaller than the aforementioned model, were also considered. The solvent (tetrahydrofuran) effect on the adduct stability as well as on the association energy in the polarizable continuum model framework was taken into account at the 6–31G* level.

Electronic Supplementary Material Supplementary material for Tables S1–S6 is available in the online version of this article at http://dx.doi.org/10.1007/s00214-003-0538-z

Keywords: BSSE – Deformation energy – Association energy – Ab initio/DFT – THF solvation

Introduction

There is a well-recognized need to obtain stereochemically pure (enantiopure) optically active compounds for a variety of uses. For instance, when using a drug as a racemic mixture, even in the most favorable case 50% of it contains active molecules and 50% useless impurities. In the worst case, the ''impurity'' may be recognized by other receptors and cause serious, even dramatic, negative effects. To prevent these kinds of problems, powerful synthetic strategies are being developed, coupled with theoretical studies aimed at improving the stereoselectivity [1, 2]. Among the chiral groups, chiral secondary alcohols are particularly important, because of their occurrence in natural compounds, and because they can easily be transformed into other functionalities with total control of configuration. The catalytic reactions (oxidations or reductions) leading to stereodefinite chiral secondary alcohols earned Sharpless, Noyori and Knowles the Nobel Prize for Chemistry in 2001.

The stereoselective reduction of carbonyl compounds can be performed with boron hydrides, in the presence of chiral catalysts. The chiral species induces hydride attack on the prochiral ketone with high facial selectivity. Itsuno

Contribution to the Jacopo Tomasi Honorary Issue

Correspondence to: G. Alagona
e-mail: G.Alagona@ipcf.cnr.it

and co-workers [3] used a mixture of borane with chiral 1,2-aminoalcohols derived from valine in defined ratios, and this mixture was capable of reducing a great variety of prochiral ketones with excellent yields and good enantiomeric excesses, particularly arylalkyl-ketones.

Corey, Bakshi and Shibata (CBS) in 1986–87 [4] proposed that the reducing agent in this case is an oxazaborolidine, and confirmed that borane coordinates to it through the nitrogen atom with X-ray measurements. However, they used proline instead of valine as starting chiral material, and simplified the preparation of the oxazaborolidine. The modified catalyst was capable of reducing a wide variety of ketones under mild reaction conditions, with quantitative yields and excellent enantiomeric excesses (see Scheme 1). Nonetheless, when a theoretical study of the acetophenone reduction by BH_3 in the presence of the CBS catalyst was attempted, substantial differences emerged in the description of the possible acetophenone-CBS-BH_3 complexes (those stable at the AM1 level are displayed in Fig. 1), depending on the method and on the basis set adopted (wide infra).

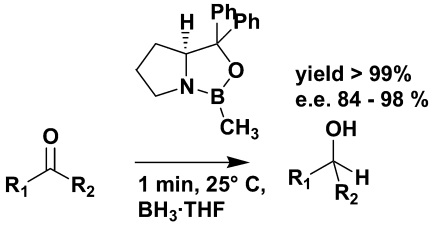

Scheme 1

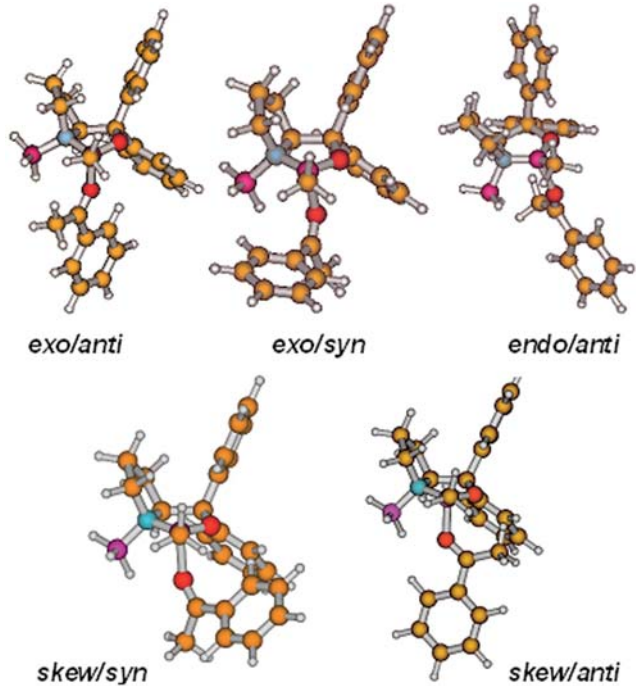

Fig. 1. Stable conformations of the acetophenone-CBS-BH_3 complexes computed at the AM1 level

This was a clear indication that not all of them are suitable for properly describing the weak ketone-oxazaborolidine interaction. A careful validation of the various methods was necessary.

Therefore, the present investigation is not focused on modeling enantioselectivity, but rather on assessing which combination of theoretical method and level is best suited to describing the interactions taking place within the complexes formed between simple models of the CBS catalyst and acetone. Because of the size of the real system, the assessment also takes into account the computational cost of the modeling. The role of the exocyclic boron hydride in the complexation of acetone is also investigated, and the interactions of acetone and two smaller Lewis bases (water and ammonia) with BH_3 are considered. Furthermore, the contribution of basis set superposition errors (BSSE) and geometry deformation to the complexation energy is taken into account. The solvent effect in the framework of the polarisable continuum model (PCM) is also considered in tetrahydrofuran (THF).

These BH_3 complexes have long been studied by a variety of methods in order to elucidate the nature of their interactions. In 1976, Umeyama and Morokuma [5] performed the interaction energy decomposition of the $BH_3\cdots NH_3$ complex, among others, at the 4–31G level in order to analyze the mutual weight of the components. Assuming that the geometry of the isolated electron donor was not altered upon complex formation, while for borane planar and pyramidal configurations were considered, they concluded that the strong binding is due to the electrostatic contribution [5]. In 1988, LePage and Wiberg studied rotational barriers for carbonyls coordinated to neutral Lewis acids (a similar scenario to BH_3-acetone), and found soft coordination modes in general [6]. Other work concerning strongly bound donor-acceptor complexes includes that by Frenking et al. who showed that the bonding in BH_3NH_3 has large covalent contributions [7], and more recently, Tomás et al. defined the bonding as intermediate between the pseudo-covalent and van der Waals types [8]. In a subsequent G2 investigation on several H_3BXH_n complexes, Tomás et al. attributed their stability to the pyramidalization of borane and to the basicity of the donor, explaining in this way the greater stability of H_3BNH_3 than H_3BOH_2 [9]. On the other hand, no investigation on BSSE has been carried out as yet, to the best of our knowledge, primarily because of the problems linked to the deformation energy [10].

Computational details

The semiempirical calculations have been carried out using the AM1 model Hamiltonian as implemented in AMSOL [11]. The source code was compiled for use on Silicon Graphics O^2 (Irix 6.5 operating system), Indigo^2 (Irix 5.3 operating system), and IBM RISC6000 workstations.

The ab initio calculations have been carried out at the Hartree-Fock (HF) and MP2 [12, 13, 14] levels, using the Gaussian 98 system of programs [15]. MP2 calculations have been performed using the frozen-core (FC) approximation. The source code was

compiled for use on a cluster of personal computers running under the Linux operating system and on DEC Alpha DS 20E Compaq workstations (Unix operating system).

Also regarding the density functional theory (DFT) framework, calculations have been carried out with Gaussian 98, using the B3LYP (Becke's three parameter hybrid functional using the LYP correlation functional [16, 17]) and MPW1PW91 (Barone and Adamo's Becke-style one parameter functional using modified Perdew-Wang exchange and Perdew-Wang 91 correlation [18]) functionals.

Several split valence-shell basis sets have been employed: 3–21G [19], 6–31G* and 6–31G** [20, 21, 22, 23], 6–31 + G** [24]. Single point calculations at the MP2, MP3, MP4SDQ, QCISD, and QCISD(T) [25] levels have been carried out on the HF/6–31G* optimized geometries.

The calculations in solution (solvent was THF) have been carried out in the PCM framework [26, 27, 28, 29]. For a detailed description, reference is made to the source papers of the method.

Model systems

In the study of the reduction of acetophenone by BH_3 in the presence of the CBS catalyst (see Scheme 1), several acetophenone-CBS-BH_3 complexes should be considered, because the coordination of borane to the catalyst, and the complexation of the ketone to the endocyclic boron, might occur for a variety of mutual arrangements of the partners. Nonetheless, the relative stability of those possible complexes are erratic [30, 31] depending on the method and on the basis set adopted. This fact clearly indicates that not all of the arrangements are able to properly describe the weak ketone-oxazaborolidine interaction.

Moreover, the HF/3–21G boron-oxygen interaction was far too negative compared to the HF/6–31G* interaction, not only because of the well-known tendency of the 3–21G basis set to overestimate electrostatic interactions, but also because of the equally well-known fact that BSSE grows as the size of the basis set decreases. It was actually reported that the complexation step is endothermic [32, 33]. In particular, Nevalainen performed scans on a model system, showing that an energy barrier prevents the energetically unfavorable complex from dissociating [32]. On the other hand, Corey stated that the ketone complexation and the highly exothermic hydride transfer are probably fast and comparably rate limiting [34, 35]. Because of these reasons, we decided to study the weak interaction responsible for the complexation of the ketone to CBS, with the aim to find the best compromise between accuracy and speed of calculations. Due to the complexity of the real system (see Fig. 1), we could not use the wide variety of methods and basis sets necessary to do a systematic study, so a model system was chosen that retained the most important characteristics involved in the B···O interaction. The side groups, important for enantioselectivity, were disregarded, because at this stage the issue of modeling enantioselectivity was outside of our scope of this work. Furthermore, for the sake of simplicity and computational speed, a nitrogen atom was used in place of the proline ring, and a proton was placed on this instead of a methyl group, despite the fact that this means that, at longer distances, acetone may reorient itself to point towards the N–H bond, because of an H-bond interaction. This interaction, that for obvious reasons cannot occur in the complete system, is a flaw in the model, and indeed it is observed when the B···O separation grows to beyond 2 Å. Nonetheless, since for this study only a region near the bottom of the potential energy well is interesting, the model is adequate since for this short B···O separation the H-bond interaction cannot take place. Furthermore, among the four possible conformers, those with acetone on the opposite face with respect to BH_3 were discarded because they did not yield a local minimum, while of the two left, the endo type structure (Fig. 2) was utilized, even though the exo type structure interaction energy was about 1.1 kcal/mol more favorable. However, a few calculations have been performed on exo type structures for comparison as well.

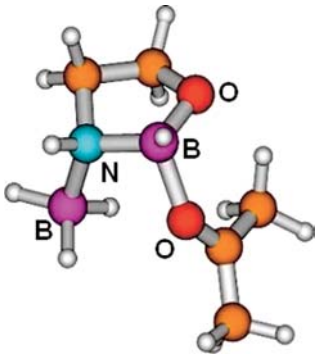

Fig. 2. Model system selected for the study of ketone-oxazaborolidine interaction

The chosen model system still contains the prominent elements of the acetophenone-CBS-BH_3 complexes: the 1,3,2-oxazaborolidine ring, to which a molecule of borane and one of acetone, the smallest possible ketone, are coordinated. As known from previous investigations, the presence of a molecule of borane coordinated to nitrogen is important because it has a considerable electronic effect on both the endocyclic boron, enhancing its Lewis acid character, and on borane itself, in that the nucleophilic character of the hydride is amplified by the electron density coming from the nitrogen lone pair. The complexation of acetone is basically due to the electrostatic interaction between a Lewis acid/base pair consisting, respectively, of the endocyclic boron and the carbonyl oxygen, joined to a significant charge transfer contribution [31]. Consequently, some electron density is drawn away from the C = O double bond, making the carbon atom more subject to hydride transfer. The presence of the ring system is important to keep the conformation rigid.

In order to better analyze the interactions taking place in the system, as well as the role of the second borane, smaller models, described in detail in the relevant sections, have been considered. In all of them, acetone, or a smaller Lewis base, coordinates to B. They can be approximately categorized into four families: 1) models without the ring system (BH_3NH_2–BHOH-acetone and BH_3NH_2–BH_2-acetone); 2) H_3B-b, with b = acetone, water, or ammonia; 3) XYHB-acetone, with either X = H and Y = OH, NH_2, or X = OH and Y = NH_2; and 4) the complex with acetone of the ring system without the exocyclic BH_3.

Results and discussion

Main model system: flexible scans along the B···O coordinate

The interaction energy along the B···O approach path for the main model system (shown in Fig. 2) at various computational levels, is displayed in Fig. 3. The relaxed scans have been carried out using several methods (HF, DFT-B3LYP, MP2) and basis sets (3–21G, 6–31G, 6–31G*, 6–31G**, 6–31 + G**), in order to evaluate the dependence of the results on the quality of the description, and to assess their reliability. The numerical data are available in the Electronic Supplementary Material, Tables S1-S3. A few comments on the trend of the curves can easily be made after observing the plots.

First, the smallest basis set considered here clearly overestimates the interaction energy. Though weaker, the interaction energy is seemingly still overestimated by the AM1 model Hamiltonian as well. In the case of HF/3–21G calculations, this is also reflected in a shorter than

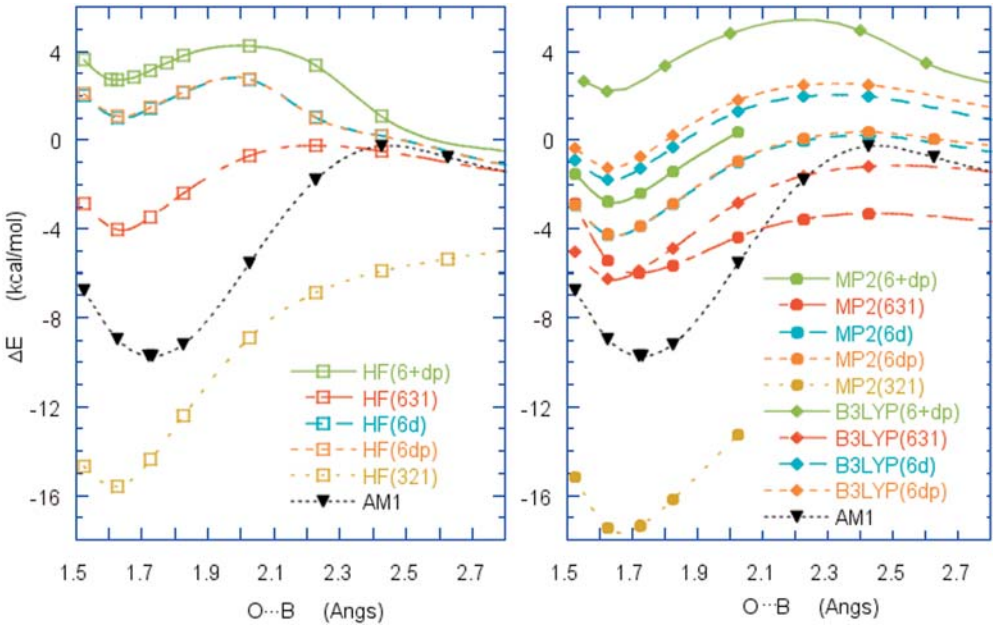

Fig. 3. AM1 interaction energy profile along the B···O approach path in the model system, shown in Fig. 2, as compared to the interaction energies obtained with various basis sets and levels of theory: HF (left hand side), MP2 or B3LYP (right hand side). 321, 631, 6d, 6dp and 6 + dp stand respectively for the 3–21G, 6–31G, 6–31G*, 6–31G** and 6–31 + G** basis sets

Table 1. B···O equilibrium separations, corresponding interaction energies (ΔE), CP corrected interaction energies[a] (ΔE^{CP}), and their components:[a] ΔE(CP), BSSE, and deformation energy (E_{def}), for all the studied combinations of method and basis set. ZPE and thermal[b]corrections (at 298.15 K) are also reported

Level	B···O (Å)	ΔE (kcal/mol)	ΔE^{CP} (kcal/mol)	ΔE(CP) (kcal/mol)	BSSE (kcal/mol)	E_{def} (kcal/mol)	ZPE (kcal/mol)	Therm[b] (kcal/mol)
B3LYP/6–31G	1.639	−6.26	−0.25	−27.03	−6.01	26.78	2.31	15.64
B3LYP/6–31G*	1.623	−1.78	3.96	−25.64	−5.75	29.60	1.66	14.19
B3LYP/6–31G**	1.623	−1.24	4.51	−25.77	−5.76	30.28	1.59	14.04
B3LYP/6–31 + G**	1.623	2.21	3.54	−25.96	−1.33	29.50	1.45	12.78
HF/3–21G	1.604	−15.63	−0.72	−31.87	−14.91	31.15	-	-
HF/6–31G	1.628	−4.02	0.24	−29.75	−4.27	30.00	2.50	15.19
HF/6–31G*	1.629	1.03	4.78	−24.62	−3.75	29.40	2.46	15.30
HF/6–31G**	1.630	1.09	4.83	−24.56	−3.74	29.40	2.46	15.34
HF/6–31 + G**	1.625	2.71	4.46	−24.85	−1.75	29.31	2.38	15.43
MP2/3–21G	1.665	−17.60	4.96	−19.63	−22.55	24.59	-	-
MP2/6–31G	1.721	−5.99	3.83	−18.30	−9.82	22.13	2.52	15.42
MP2/6–31G*	1.640	−4.27	5.40	−24.13	−9.66	29.53	1.45	13.68
MP2/6–31G**	1.640	−4.26	5.26	−24.76	−9.52	30.02	1.45	13.76
MP2/6–31 + G**	1.639	−2.77	4.04	−25.72	−6.82	29.76	1.18	13.56

[a] These values correspond to the uncorrected equilibrium positions, not to the CP corrected minima
[b] including ZPE

normal B···O distance, whereas longer than normal B···O separations are found at the MP2/3–21G level, and especially at the AM1 level, as can be seen by looking at the data reported in the first column of Table 1. The 6–31G description represents a considerable improvement with respect to the 3–21G one, as expected, at least as far as the interaction energy is concerned.

Second, a remarkably different behavior is obtained when polarization functions are added. By comparing the practically superimposed 6–31G* and 6–31G** curves, however, it is evident that the addition of *p* polarization functions on hydrogens cause almost no change. From this finding, common to HF, B3LYP and MP2 calculations, it can be inferred that, while *d* polarization functions are necessary to give a different (and presumably better) description of the system, the *p* polarization functions do not produce significant improvement. The main observed influence of polarization functions is to further reduce the interaction energy so that, in the case of HF calculations, it becomes positive. Therefore, the two partners turn out to be less stable in the complex than at infinite separation.

The third comment is that, after introducing *sp* diffuse functions on heavy atoms, the complex is further destabilized, to the point that a negative interaction energy with the 6–31 + G** basis set is predicted only at the MP2 level.

It is worth noting that, although the interaction energies for some basis sets are positive, for all the calculated complexes a local minimum can be found at a

sensible equilibrium separation. In fact, increasing the B···O distance over a short range increases the energy of the endothermic complex, indicating that there is an energy barrier to dissociation. The B3LYP behavior is intermediate between the HF and MP2 ones, though with a larger gap than that found using HF and MP2 among the various basis sets.

While it is not completely known whether and how much the quality of the description is improved by the addition of *sp* diffuse functions, it is likely from the interaction energy/basis set trend that BSSE, described in the next section, plays a prominent role in this kind of system.

BSSE

The most popular counterpoise procedure (CP) to correct basis set superposition errors, proposed by Boys-Bernardi [36], was intended for van der Waals complexes, with the hypothesis that intermolecular interactions do not affect the internal geometries of the partners. Conversely, Jansen-Ros [37] applied the correction to the protonation of CO with relaxed interatomic distance. The use of flexible geometries, optimized along the approach coordinate in the dimer, instead of rigid geometries, complicates matters. Though the equations can be found in a previous article [38], in order to make the paper self-contained and define the various quantities we make reference to, we report a short derivation of the equations employed.

The interaction energy at the X level (with X = HF, B3LYP or MP2 in the present case) is given by:

$$\Delta E^{\mathrm{X}} = E^{\mathrm{X}}(\mathrm{AB}) - E^{\circ\mathrm{X}}(\mathrm{A}) - E^{\circ\mathrm{X}}(\mathrm{B}) \tag{1}$$

where $E^{\circ\mathrm{X}}(\mathrm{M})$ is the energy of the isolated monomers (A or B) at the X level in a given geometry (usually that optimized at infinite separation). For the sake of simplicity, the indication of the level (X), which is supposed to be the same on both sides of the equations, is omitted from now on.

To make clear which geometry and which basis functions are used, Eq. 1 can be written as:

$$\Delta E = E(\mathrm{AB}) - E^{\mathrm{m,m}}(\mathrm{A}) - E^{\mathrm{m,m}}(\mathrm{B}) \tag{2}$$

where in $E^{\mathrm{m,m}}(\mathrm{M})$ the first superscript stands for the geometry of M, m (optimized in the monomer), and the second superscript for the basis functions, m (of the monomer). When the monomers get closer and closer, their charge distributions are polarized and this affects their equilibrium nuclear positions, if geometry deformation is allowed. The deformation contribution is given by:

$$E_{\mathrm{def}} = E^{\mathrm{d,m}}(\mathrm{A}) - E^{\mathrm{m,m}}(\mathrm{A}) + E^{\mathrm{d,m}}(\mathrm{B}) - E^{\mathrm{m,m}}(\mathrm{B}), \tag{3}$$

where $E^{\mathrm{d,m}}(\mathrm{M})$ is the energy of the monomer computed with the geometry of M optimized in the dimer and the monomer basis functions. Therefore ΔE accounts for deformation as well:

$$\Delta E = E_{\mathrm{int}} + E_{\mathrm{def}} \tag{4}$$

$$\text{with} \quad E_{\mathrm{int}} = E(\mathrm{AB}) - E^{\mathrm{d,m}}(\mathrm{A}) - E^{\mathrm{d,m}}(\mathrm{B}) \tag{5}$$

The assumption of the counterpoise procedure is that the energy of the reference state must be modified to avoid the artificial stabilization of the complex. The correction is made taking as reference energy the two partners at a definite distance, each in the presence of the basis functions of the other, as they are in the adduct, instead of considering them at infinite separation. Since the CP correction consists of a change in the reference energies, when the geometry of M optimized in the monomer with the dimer basis functions is used to compute the energy of the monomers (in other words $E^{\mathrm{m,d}}(\mathrm{M})$), if we employ rigid geometries there is no contribution from deformation (the first index is just included for comparison):

$$\Delta E(\mathrm{CP}) = E(\mathrm{AB}) - E^{\mathrm{m,d}}(\mathrm{A}) - E^{\mathrm{m,d}}(\mathrm{B}). \tag{6}$$

According to Sokalski et al. [39], BSSE can be directly defined as ΔE–ΔE(CP):

$$\mathrm{BSSE} = E^{\mathrm{m,d}}(\mathrm{A}) + E^{\mathrm{m,d}}(\mathrm{B}) - E^{\mathrm{m,m}}(\mathrm{A}) - E^{\mathrm{m,m}}(\mathrm{B}). \tag{7}$$

The geometry deformation treatment for the interacting partners is not necessary when feeble intermolecular interactions are considered, but it becomes more and more important when reactive interactions are studied. In the past, due to limited computational power, theoreticians were forced to use rigid geometries for the construction of CP-corrected interaction energy profiles, whereas a flexible scan should be employed. However, the inclusion of a deformation energy term into BSSE may result in totally wrong numbers, especially when the geometries of the partners undergo considerable variations as a consequence of strong interactions. Even in the last few years, the occurrence of this problem has been mentioned only sporadically [38, 40, 41, 42].

In analogy with Eqs. 6 and 7, when the geometries are relaxed:

$$\Delta E(\mathrm{CP}) = E(\mathrm{AB}) - E^{\mathrm{d,d}}(\mathrm{A}) - E^{\mathrm{d,d}}(\mathrm{B}) \tag{8}$$

$$\text{and} \quad \mathrm{BSSE} = E^{\mathrm{d,d}}(\mathrm{A}) + E^{\mathrm{d,d}}(\mathrm{B}) - E^{\mathrm{d,m}}(\mathrm{A}) - E^{\mathrm{d,m}}(\mathrm{B}). \tag{9}$$

The difference between ΔE and ΔE(CP), easily derivable, consists of two terms, one related to BSSE and the other to geometry deformation (Eq. 3) [38]:

$$\Delta E - \Delta E(\mathrm{CP}) = \mathrm{BSSE} + E_{\mathrm{def}}. \quad (10)$$

In the case of flexible geometries, therefore, the CP-corrected interaction energy, ΔE^{CP}, can be obtained using either expression:

$$\Delta E^{\mathrm{CP}} = \Delta E - \mathrm{BSSE} = \Delta E(\mathrm{CP}) + E_{\mathrm{def}} \quad (11)$$

The CP-corrected interaction energies, ΔE^{CP}, reported together with BSSE and E_{def} in Table 1, are decidedly less favorable than the uncorrected ones (also displayed), but the largest effect is due to the deformation term, that ranges from 22 to 31 kcal/mol in the region of the uncorrected minimum. This large effect is primarily ascribable to the distortion in the oxazaborolidine ring, because the hybridization of the endocyclic B atom changes from sp^2 (planar geometry) to sp^3 (tetrahedral geometry). However, since the CP-corrected energy interaction profile is smoother than the uncorrected one, while the minimum is likely to be situated at a longer distance, the application of the CP correction only at the uncorrected equilibrium distance produces an exaggerated destabilization in the interaction energy, that may assume even positive, non-bonding values. For this reason, it is more appropriate to compute the correction along the whole approach path [43] in order to find energy and equilibrium distance at the bottom of the CP-corrected curve.

From inspection of the relaxed, CP-corrected scans reported in Fig. 4, the importance of both BSSE and E_{def} is immediately evident. All corrected interaction energies at equilibrium (ΔE^{CP}) are positive or very close to zero, in contrast to the uncorrected (ΔE) curves, where in the majority of cases the energy at the bottom of the curve has a negative sign, whereas the ΔE(CP) curves (not displayed), have minima at even more negative values than the uncorrected ΔE curves.

From the comparison between basis sets, within the three sets of methods (HF, B3LYP and MP2) no large differences emerge in the description when using basis sets above the 6–31G* one. Therefore, it seems advisable to resort to the cheapest of the upper-quality basis sets (the 6–31G* basis set) for the subsequent investigation of the complete system [30, 31]. Furthermore, while it is desirable to select a method that avoids gross errors, it must be kept in mind that for the prediction of the stereochemical outcome, the relative and not the absolute energy is important.

In addition, once again basis sets not containing polarization functions behave differently, showing exceedingly stable minima and long B···O equilibrium distances, while the gap between polarized basis sets and those also containing *sp* diffuse functions is inverted in sign with respect to the uncorrected curves, and reduced in amplitude. This is due to the very small error affecting the 6–31 + G** basis set: it is worth noticing that after correction the interaction energies at the equilibrium distance are fairly close to each other regardless of the calculation method. The poor performance of the limited basis sets is particularly evident at the MP2 level: the 3–21G B···O equilibrium distance is extremely long, while the 6–31G curve is even smoother.

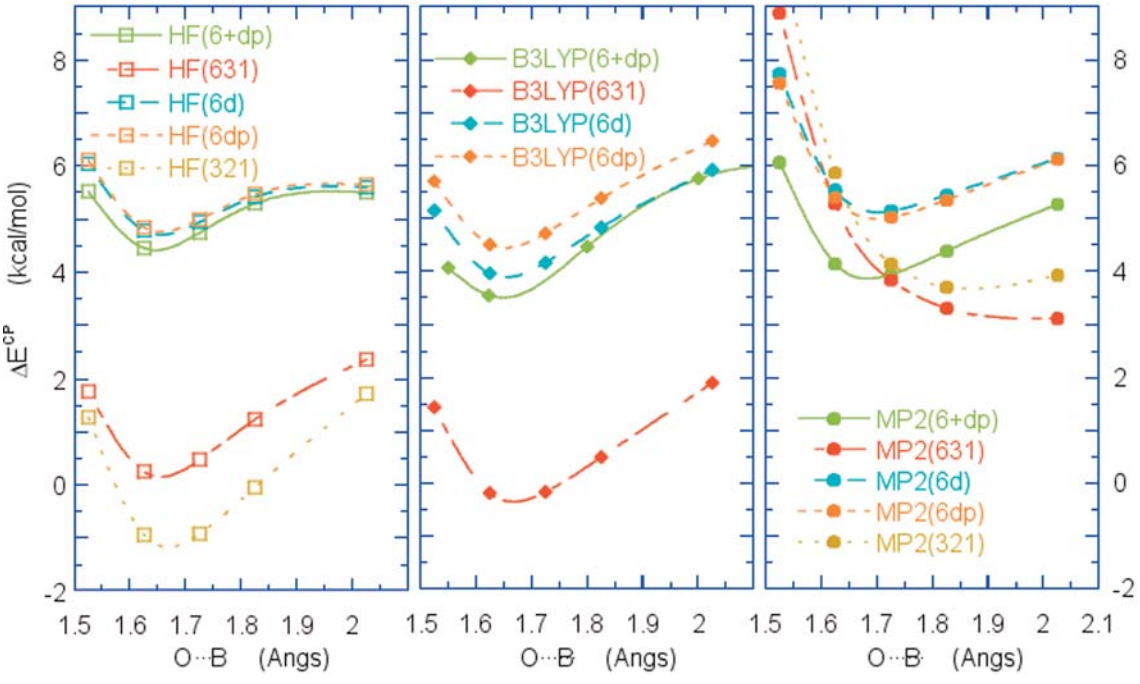

Fig. 4. Relaxed geometry CP-corrected interaction energy profiles along the B··O approach path in the model system, shown in Fig. 2, at various levels of theory: HF, B3LYP and MP2. Basis set legends as in Fig. 3

Smaller models

Oxazaborolidine-borane

Another hint that 6–31G* is the smallest basis set among those having superior descriptive quality comes from calculations carried out for the oxazaborolidine-borane (OAB-BH_3) system (shown in Fig. 5). In this system, the sp^2 B atom can interact with a hydride, forming a three-center, two-electron bond, similar to that present in gaseous diborane, and also encountered in some computational works on oxazaborolidines [32]. Therefore, such a structure can be considered a distinctive feature if a method is able to produce it or not. As the interaction becomes more intense, the B atom is forced out of planarity and changes its character from sp^2 to sp^3. The hybridization change can be put forward by the value of the H–B_2–N–C dihedral angle, while the out of plane distortion of B is given by the value of the H–B_2–N–O improper dihedral angle.

Since this system is not symmetric, and because of the conformational restraints imposed by the oxazaborolidine ring, the strength of the three-center, two-electron interaction is probably weaker than in diborane. On a qualitative basis, the more stretched the bond between the exocyclic B atom and the hydride, compared to the other two, the stronger the hydride interaction with the endocyclic B atom. Analogously, the interaction is enhanced when the B···H···B system is more symmetric. Geometry optimizations of the OAB-BH_3 complex were carried out using the same combinations of methods and basis sets as used for the B···O interaction study.

The relevant geometric data, reported in Table 2, confirm that 6–31G* geometries are qualitatively very different from those obtained using smaller basis sets, at least at the B3LYP and MP2 levels, but very similar to those obtained with larger basis sets. It is even possible from these data to find a further distinction between the methods. The HF level, even though it uses large basis sets, fails to predict the bridged hydride interaction. Seemingly, to properly describe the system in the gas phase, electron correlation effects must be taken into account to some extent. The portion of correlation energy recovered at the MP2 level, and even at the B3LYP one (though the latter cannot account for dispersion interactions), is enough to give a qualitatively superior description.

The occurrence of a bridged hydride interaction, however, somewhat influences the magnitude of the coordination energies displayed in Fig. 3 (right hand side) and in Fig. 4, as we will discuss later.

As far as the 6–31 + G** basis set is concerned, in general the addition of *sp* diffuse functions considerably affects the energy profiles with respect to those obtained using the basis sets with polarization functions.

Borane-b (with b = water, ammonia, acetone)

The calculations on the smallest models considered here, only composed of BH_3 and a simple Lewis base, have been carried out with the full combination of basis sets and methods – the same as those used for the main model system – in order to evaluate their performance as well as the change in the BSSE effect related to the system size. The AM1 results are displayed together with the uncorrected values for comparison.

The $H_3B{\cdots}OH_2$ interaction energy along the B···O approach path is shown in Fig. 6 at the various uncorrected levels. The behavior of the basis sets for the HF and MP2 methods is fairly consistent with that obtained for the main model system, though the interaction strength is considerably stronger than previously. Conversely, B3LYP produces results closer to MP2, especially for the most extended basis sets (6–31G*, 6–31G**, and 6–31 + G**). Considering the 6–31G* basis set, $\Delta E \sim -9$ or –18 kcal/mol, respectively, at the HF or B3LYP/MP2 levels, versus –21 kcal/mol obtained with AM1, that in addition shows steep walls; in the attractive branch even steeper than the 3–21G ones. This is a general feature of AM1 for all of the systems con-

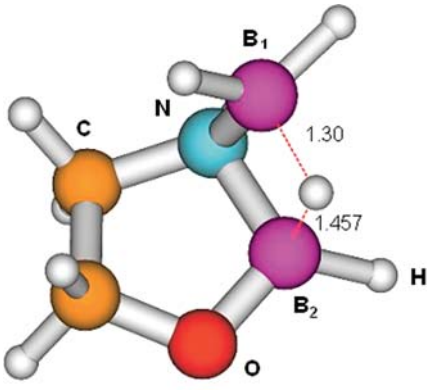

Fig. 5. B3LYP/6–31G* optimized geometry of the oxazaborolidine-borane complex

Table 2. Values of the HB_2NC and HB_2NO dihedral angles (in degrees) in the OAB-BH_3 complex optimised at different levels of theory

Level	HB_2NC	HB_2NO
B3LYP/6–31G	163.7	177.1
B3LYP/6–31G*	139.8	144.0
B3LYP/6–31G**	139.6	143.7
B3LYP/6–31 + G**	139.6	143.6
HF/3–21G	164.7	178.3
HF/6–31G	164.5	178.3
HF/6–31G*	163.2	178.3
HF/6–31G**	163.3	178.3
HF/6–31 + G**	163.4	178.4
MP2/3–21G	163.9	178.4
MP2/6–31G	163.3	178.3
MP2/6–31G*	138.8	141.9
MP2/6–31G**	139.0	142.1
MP2/6–31 + G**	139.2	142.1

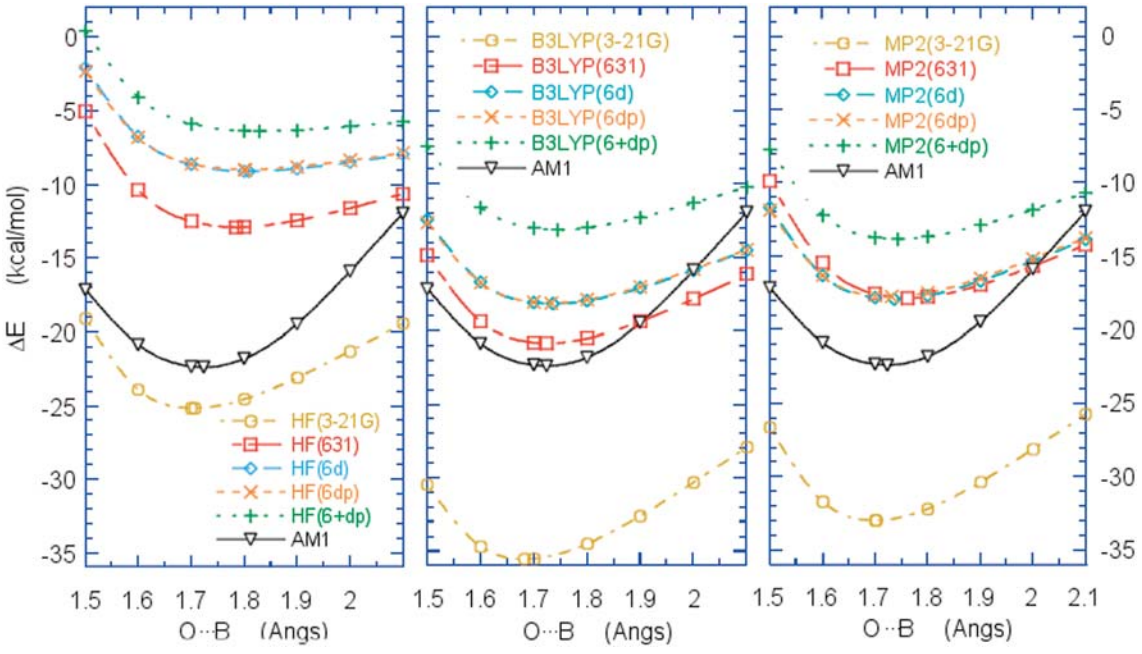

Fig. 6. Relaxed geometry interaction energy profiles along the B··O approach path in $H_3B{\cdots}OH_2$ at various levels of theory: HF, B3LYP and MP2. Basis set legends as in Fig. 3

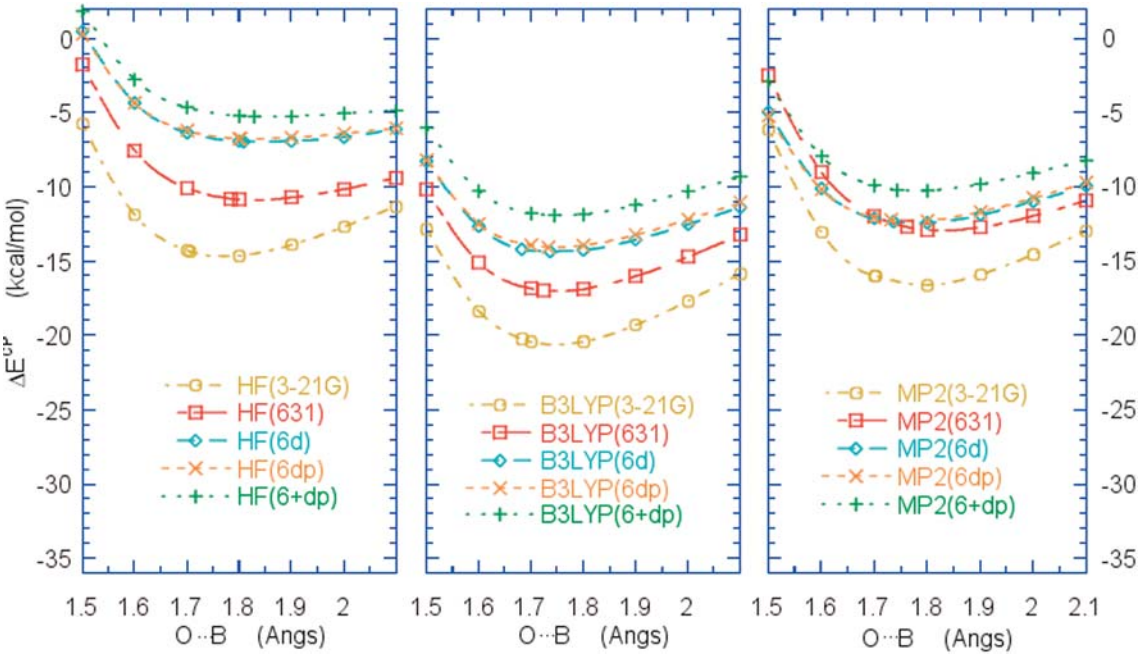

Fig. 7. Relaxed geometry CP-corrected interaction energy profiles along the B··O approach path in $H_3B{\cdots}OH_2$ at various levels of theory: HF, B3LYP and MP2. Legends as in Fig. 3

sidered here. Interestingly enough, the AM1 equilibrium distance is close to those of B3LYP and MP2. At the MP2 level, the 6–31G interaction energy is almost superimposed on the 6–31G* and 6–31G** ones, though it is slightly less favorable in the repulsive branch, producing a somewhat longer equilibrium separation. This trend is maintained as well at the CP-corrected level. After CP corrections (Fig. 7) the complexes are, in general, significantly less stable than at the corresponding uncorrected level, as expected, while the spreading of the curves is greatly reduced. Nonetheless the equilibrium distances still correspond to reasonably strong interaction energies ($\Delta E \sim -7$, -14 or -12 kcal/mol, respectively, at the HF, B3LYP or MP2 levels).

From the inspection of the $H_3B{\cdots}NH_3$ curves displayed in Fig. 8, analogous conclusions can be drawn,

even though for this system the coordination energy is much stronger (ΔE∼–23.5, –32.8, or –34.4 kcal/mol, respectively, at the HF, B3LYP, or MP2 levels, versus –38.3 kcal/mol obtained with AM1 at 1.5616 Å). Notice that this is a much shorter equilibrium separation than those found with the other methods, perhaps indicating the need for further improvement in the B-N parameterization). The behavior of the basis sets for the HF and MP2 methods is similar, although the interaction strength is about 10 kcal/mol stronger at the MP2 level than at the HF one. The spread in the curves is enhanced with B3LYP: the 3–21G and 6–31G profiles show a greater stability than at the MP2 level, whereas the 6–31G*, 6–31G**, and 6–31 + G** profiles correspond to a lower stability.

Interestingly, the B3LYP/6–31G* minimum occurs at a B···N separation of 1.669 Å, while the B3LYP/6–31G** minimum (–32.4 kcal/mol) occurs at 1.668 Å. These values are close to the MP2/6–31 + G** values (complexation energy = –30.95 kcal/mol at 1.662 Å), with experimental values of –31.1 kcal/mol [44] and 1.657 Å [45]. The reduced stabilities obtained after CP corrections (shown in Fig. 9, $\Delta E\sim$ –21.0, –29.7 or –28.2 kcal/mol, respectively, at the HF, B3LYP or MP2/6–31G* levels), nonetheless, remain in fair agreement with the experimental values as far as B3LYP and MP2 are concerned.

Similar remarks can be made about the $H_3B{\cdots}O=C(CH_3)_2$ complex (shown in Fig. 10). With the 6–31G* basis set we get ΔE∼–9.2, –19.5 or –18.8 kcal/mol, respectively, at the HF, B3LYP or MP2 levels, versus –18.7 kcal/mol obtained with AM1, although for this system AM1 gives a longer equilibrium separation (1.7178 Å). At the CP-corrected level (shown in Fig. 11), the most extended basis set (6–31 + G**) is bunched together with 6–31G* (ΔE ∼–7.3, –16.7 or –13.5 kcal/mol, respectively, at the HF, B3LYP or MP2 levels) and 6–31G**, whereas the basis sets without polarization functions not only come close (HF) and reach (B3LYP), but are even overcorrected (MP2) with respect to the more extended ones. Interestingly enough, for whatever method, CP-corrected or not, the absence of polarization functions corresponds to longer equilibrium distances.

As a common feature, the B3LYP interaction energies are the most favorable ones, CP-corrected or not.

The effect of substituents, similar to those found in the oxazaborolidine ring system, replacing some of the borane hydrogens, was then considered. All of the forthcoming models were computed only at the CP-uncorrected HF and B3LYP/6–31G* levels, because at this point we are not interested in the absolute value, but rather in the effect produced by any change in the model. In addition, for medium size models intermediate behavior of the CP correction can be assumed.

$X–H_2B{\cdots}O=C(CH_3)_2$

When X = OH, in other words when an hydroxy group replaces one of the borane hydrogens, this single substitution produces a considerable effect, as can be seen by comparing Fig. 12 to Fig. 10. Though the repulsive branch is similar, the attractive one monotonically (but

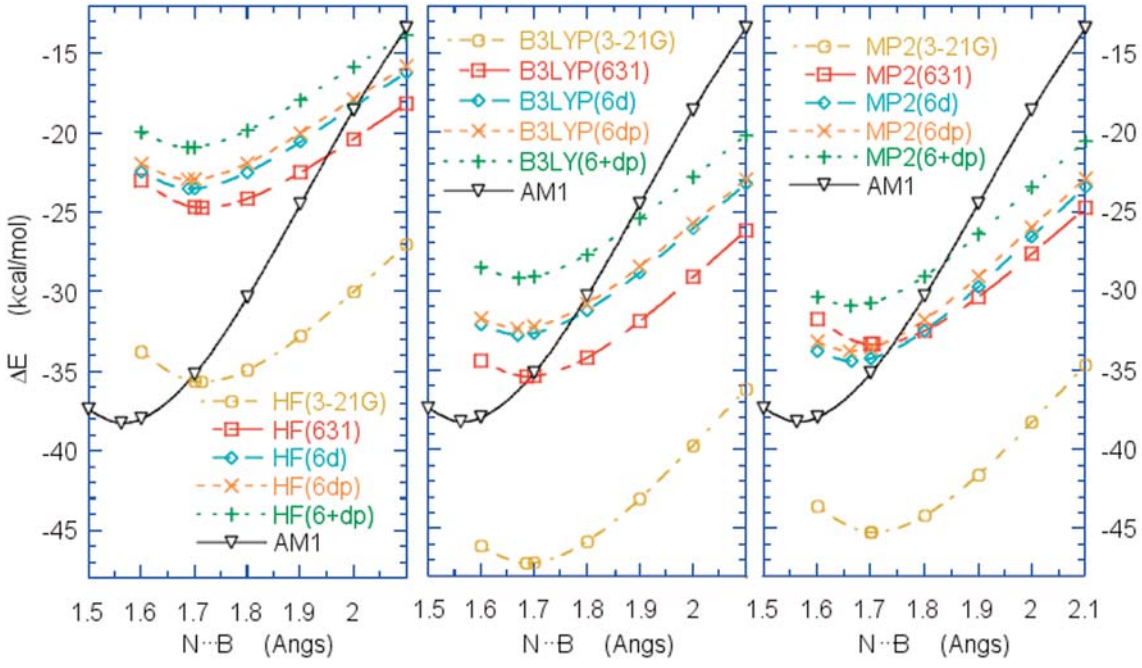

Fig. 8. Relaxed geometry interaction energy profiles along the N···B approach path in $H_3B{\cdots}NH_3$ at various levels of theory: HF, B3LYP and MP2. Basis set legends as in Fig. 3

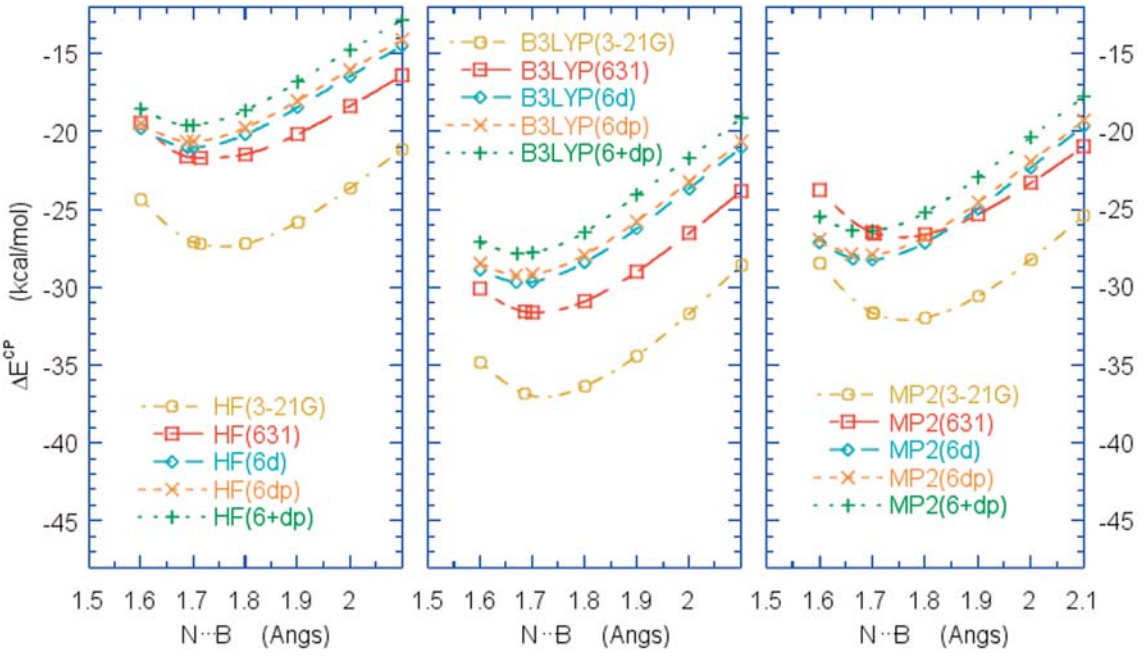

Fig. 9. Relaxed geometry CP-corrected interaction energy profiles along the N···B approach path in $H_3B{\cdots}NH_3$ at various levels of theory: HF, B3LYP and MP2. Legends as in Fig. 3

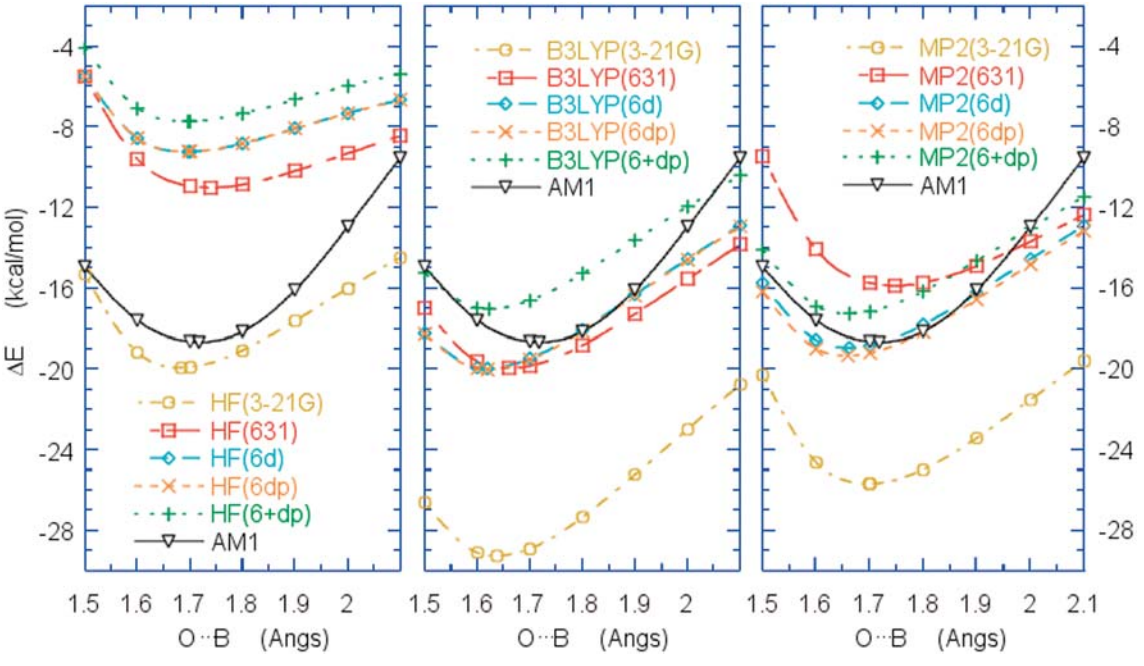

Fig. 10. Relaxed geometry interaction energy profiles along the O···B approach path in $H_3B{\cdots}OC(CH_3)_2$ at various levels of theory: HF, B3LYP and MP2. Legends as in Fig. 3

very slowly) decreases. In addition, while the B3LYP interaction energy is favorable in the region of the former minimum ($\Delta E{\sim}$–3 kcal/mol), the HF/6–31G* value is positive by a couple of kcal/mol. The effect on the complexation energy when $X = NH_2$, in other words when an amino group replaces one of the borane hydrogens, also shown in Fig. 12, is even worse. Both the HF and B3LYP/6–31G* interaction energies are unfavorable. The interaction energies decrease at long separations because the acetone carbonyl can eventually become involved in H-bonds to the hydroxy or amino hydrogens.

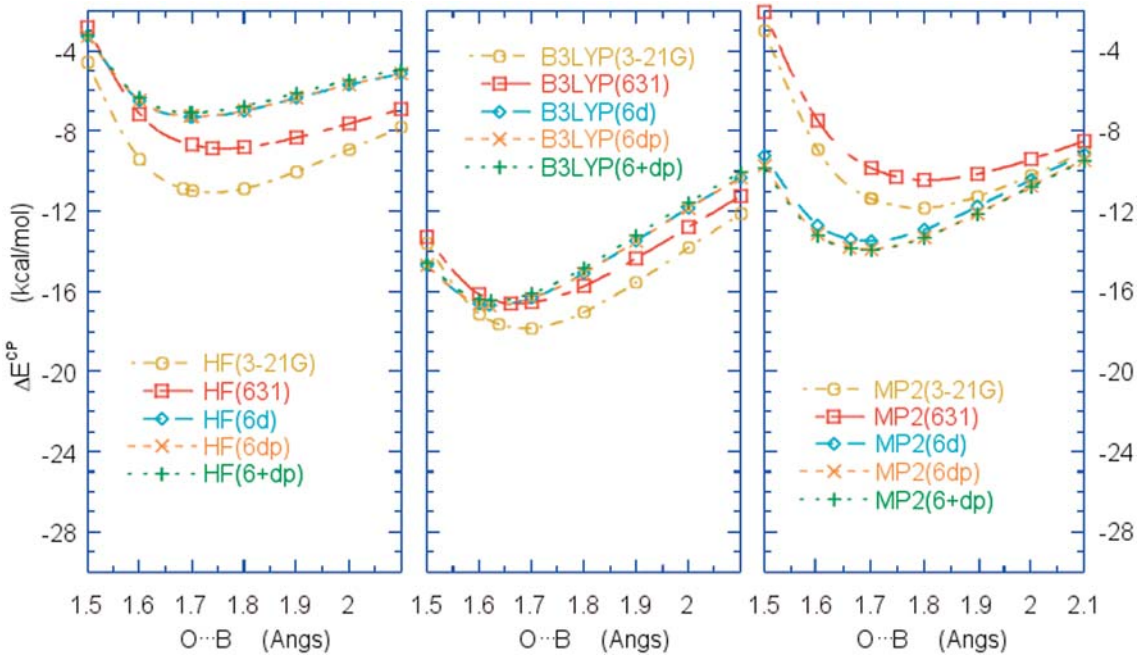

Fig. 11. Relaxed geometry CP-corrected interaction energy profiles along the O···B approach path in $H_3B{\cdots}OC(CH_3)_2$ at various levels of theory: HF, B3LYP and MP2. Legends as in Fig. 3

$HXYB{\cdots}O=C(CH_3)_2$

The trend of the $H(NH_2)(OH)B{\cdots}$acetone interaction at the HF and B3LYP/6–31G* levels is also shown in Fig. 12. The simultaneous presence of both the hydroxy and amino substituents at B produces a noticeable worsening in the complexation energies, that become by far the least favorable ones.

Ring system (without the exocyclic BH_3) $\cdots O=C(CH_3)_2$

Similar behavior is also obtained for the ring system of Fig. 5 in the absence of the exocyclic BH_3. The relevant curves, also displayed in Fig. 12, are slightly less unfavorable than those obtained for the complex $H(NH_2)(OH)B{\cdots}$acetone, probably because the substitution of two polar hydrogens with a $-CH_2-CH_2-$ group, apart from introducing structural constraints, does not greatly affect the charge distribution at B.

Role of the second BH_3

The comparison between the trend in Fig. 12 and the corresponding one in Fig. 3 clearly indicates that the second BH_3, linked to the amino group, is necessary in order to stabilize the complex. This holds for the complexes with acetone of NH_2–BH_2 and H_2N–BHOH as well, as can be seen by comparing the relevant plots in Fig. 13 with those shown in Fig. 12. Furthermore, the presence of the hydroxy group greatly affects the complex stability, even though for that system just a shallow minimum is found.

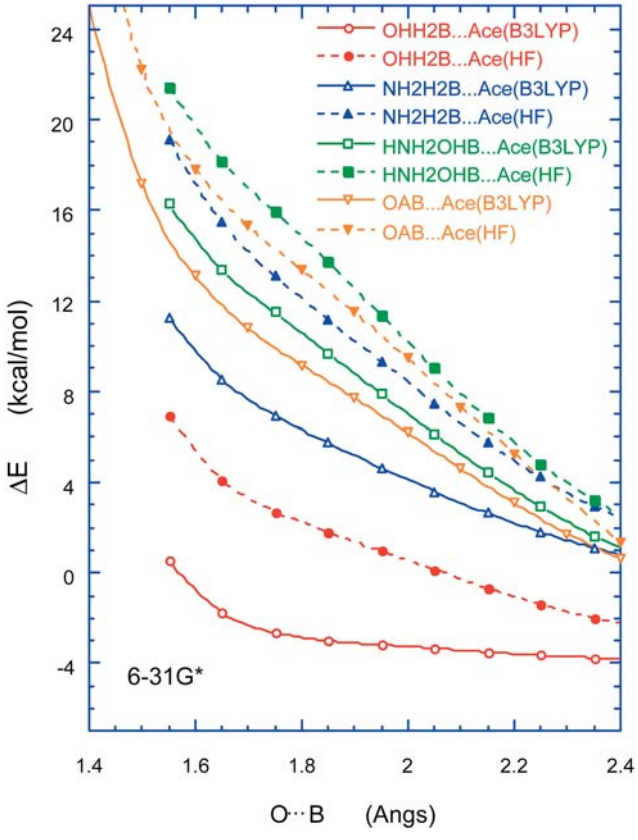

Fig. 12. Relaxed geometry interaction energy profiles along the O···B approach path in various complexes with acetone of BH_2OH, BH_2NH_2, $BHOHNH_2$, and oxazaborolidine (OAB) at the HF and B3LYP/6–31G* levels

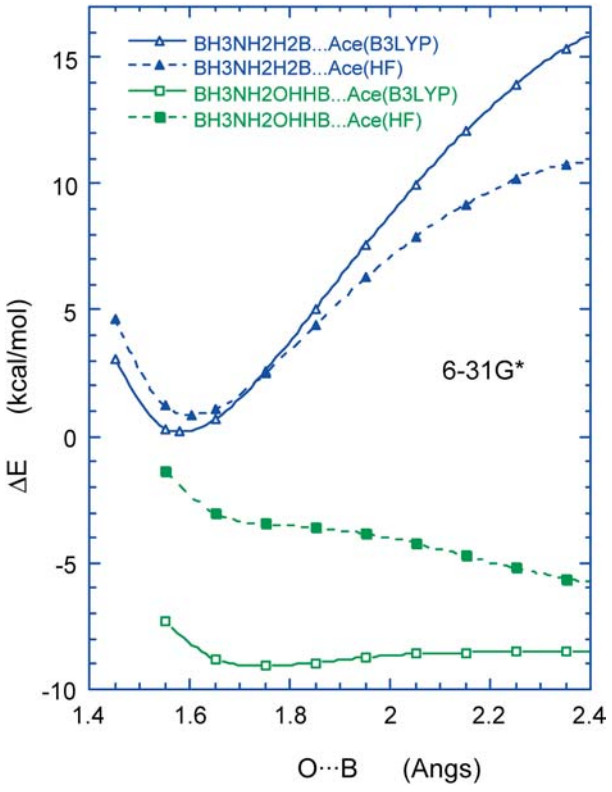

Fig. 13. Relaxed geometry interaction energy profiles along the O···B approach path for complexes with acetone of BH_2NH_2 and $BHOHNH_2$ in the presence of a BH_3 at N, at the HF and B3LYP/6–31G* levels

Main model system: energies and geometries

The analysis carried out so far gives a fairly consistent picture of the interactions taking place in oxazaborolidine. There are however a few points to be clarified concerning the complex stability.

The amount of the free energy contribution in the gas phase

Zero point energy (ZPE) and thermal corrections (including ZPE) to the association energy, computed at the HF and B3LYP/6–31G, 6–31G*, 6–31G**, and 6–31 + G** levels, are also reported in Table 1. B3LYP results are fairly consistent with the MP2 ones, as shown in the case of F-uracil dimers [46]. The frequency calculations confirmed that the corresponding complexes are local minima, as expected, with the only exception being acetone at the B3LYP/6–31 + G** level that even after a very tight optimization produced an imaginary frequency. This fact is highlighted in the thermal corrections, that turn out to be lower by about 1 kcal/mol than in the other cases, because the imaginary frequency was discarded, reducing the vibrational entropy from 10–11 to 6 cal/mol K. Actually, the two lowest frequencies correspond, respectively, to disrotatory and conrotatory modes of the methyl groups. However, it is difficult to say whether these torsions are really vibrations or hindered rotations [47]. Nonetheless, the B3LYP/6–31 + G** lowest energy arrangement of acetone, with one of the Hs for both methyl groups *syn* with respect to the carbonyl O, corresponds to a minimum with all the other basis sets (at the HF level with all basis sets here considered). The inability to produce all positive eigenvalues of the Hessian matrix is seemingly linked to the combined use of B3LYP and *sp* diffuse functions, in that a similar behavior was obtained at the B3LYP/6–311 + + G** level for acetone [49]. Interestingly enough, B3LYP/6–31 + G** geometry optimizations of acetone, starting with both methyl groups rotated by 180° with respect to the lowest energy arrangement, converged to an almost unaltered structure (higher in energy by ~1.8 kcal/mol) with two imaginary frequencies, whereas the barrier to rotation of one methyl group while keeping the other *syn* with respect to the carbonyl oxygen is only about 0.5 kcal/mol. Therefore, a much steeper path is obtained when both methyl groups rotate.

ZPE values were not scaled. When frequency scaling factors are available, as for the B3LYP/6–31G* [50] and HF/6–31G* [51] levels, the scaled ZPE values turn out to be lower, respectively, by 0.032 and 0.212 kcal/mol with relevant thermal corrections of 14.16 and 15.09 kcal/mol. The free energy balance in the association process is almost constant and rather unfavorable due to the loss of isolated partner translational and rotational degrees of freedom. Taking into account the values obtained on average at the HF level from now on, that are very similar to the B3LYP and MP2 ones (see Table S4 in the electronic supplementary material), contributions of 62 and 65 cal/mol K respectively for the acetone and OAB-BH_3 isolated partners become 70 cal/mol K in the complex. This entropy loss (amounting to 57 cal/mol K) is only partially recovered because of the presence of six new internal degrees of freedom of the complex [52]. Actually, we find vibrational entropy contributions of 11 and 12 cal/mol K for the acetone and OAB-BH_3 isolated partners that become 34.5 cal/mol K in the complex.

The effect of the isolated partner structure

The arrangement of the isolated partners does not represent a particular problem as far as acetone is concerned, in that acetone undergoes limited changes in the association process (discussed below in the section concerning solvent effects); furthermore they are fairly comparable regardless of the combination of basis set and method used. On the other hand, as stated in the oxazaborolidine-borane section, in the gas phase the oxazaborolidine-borane part takes two distinct structures, according to the basis/method combination used in this study: an open structure at the AM1 and HF levels, as well as at the B3LYP and MP2 levels when basis sets without polarization functions are used; and a closed structure (with a hydrogen bridged between the

two B atoms) at the B3LYP and MP2 levels with the 6–31G*, 6–31G** and 6–31 + G** basis sets. The main consequence of this fact is a somewhat less favorable association energy in the second case, because of the considerable stability of the closed structure with respect to the open one, which is also taken in the complex. There is no simple way to account for this. Probably, in solution a complex with the solvent (THF) is formed, preparing the oxazaborolidine-borane catalyst for the ketone interaction, but it is difficult to take this additional interaction into account, even if considering a ternary system made up of acetone, oxazaborolidine-borane and THF.

A straightforward way to evaluate the influence of the isolated partner structure on the adduct association energy is to consider the approaching pathway at the MP2/6–31G* level, albeit using the HF/6–31G* geometries that, as mentioned above, feature a very similar geometry for the isolated catalyst to that for the coordinated one. The resulting plot is displayed in Fig. 14, together with the corresponding curves up to the QCISD(T) level. The HF/6–31G* curve, already shown in Fig. 3 (left hand side), is also reported for comparison. The trend of the MP2/6–31G* coordination energy is consistent with that shown in Fig. 3 (right hand side) which was obtained using the MP2/6–31G* optimized geometries. The obvious difference however is in the equilibrium value of the coordination energy, which is about twice as favorable as the value reported in Fig. 3. This difference is primarily ascribable to the energy gain in the isolated structure of oxazaborolidine-borane because of the bridged H. The relevant geometrical parameters are: B_1–H = 1.30 Å, B_2–H = 1.42 Å, $\angle B_1$–H–B_2 = 91.8° and B_1–H = 1.21 Å, B_2–H = 2.67 Å, $\angle B_1$–H–B_2 = 71.1° at the MP2/6–31G* and HF/6–31G* levels, respectively, where B_1 is the exocyclic boron. In the coordinated structure, at the MP2/6–31G* level, those values become: B_1–H = 1.21 Å, B_2–H = 3.00 Å, $\angle B_1$–H–B_2 = 67.4°. The MP3 curve is about 1.1 kcal/mol less favorable than the MP2 one in the minimum, while it is slightly less favorable in the attractive branch and somewhat more favorable in the repulsive branch. The MP4SDQ, QCISD, and QCISD(T) curves are parallel (at least in the B···O range 1.5–1.9 Å), with MP4SDQ and QCISD producing adducts slightly less stable than MP3. Conversely, QCISD(T) almost matches MP2, that gives the most favorable values.

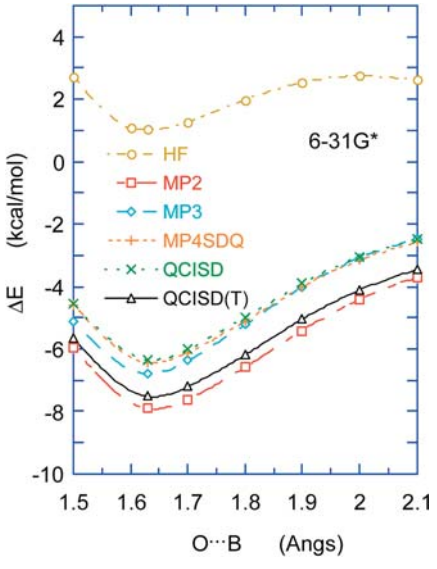

Fig. 14. 6–31G* interaction energy profiles along the O···B approach path for complexes with acetone of oxazaboroline in the presence of a BH_3 at N, calculated at different levels on the HF/6–31G* optimised geometries

The solvent effect

The solvent effect, G_{sol}, including non-electrostatic terms, on the adduct energy was evaluated in the PCM framework, with full geometry optimization in THF solution ($\epsilon = 7.58$) of the complex along the B···O approaching path at the HF and B3LYP/6–31G* levels:

$$G_{sol} = G_{SCF} - E_{vac}. \tag{12}$$

As far as the optimization strategy in solution is concerned, details can be found in [53]. Even in THF solution, the exo conformers turned out to be more favorable than the endo ones, with a solvent free energy contribution, G_{sol}, somewhat larger for exo than for endo geometries, though both kinds of structures are local minima.

The MP2 calculations in THF solution have been carried out at the MP2/6–31G* level on three different geometries: on the HF/6–31G*structures obtained in vacuo (MP2/6–31G*//HF(vac)/6–31G*); on the HF/6–31G* structures obtained in THF solution (MP2/6–31G*//HF(THF)/6–31G*), and on the MP2/6–31G* structures obtained in vacuo (MP2/6–31G*//MP2(vac)/6–31G*).

The solvent effect on the endo structures, reported in Table 3, is displayed in Fig. 15 after addition to the interaction energy in vacuo:

$$\Delta G = \Delta E + G_{sol}. \tag{13}$$

No CP or thermal corrections in vacuo are included, to allow the interested reader to combine them at will. The largest solvent effect is found at the HF level, and then at the B3LYP one, which is closely followed by MP2 on the MP2(vac) structures. This explains the noticeable stability gain in solution in the case of HF, B3LYP and MP2//MP2(vac) adducts as compared to the corresponding curves in vacuo, shown in Fig. 3. Conversely, the G_{sol} obtained at the MP2 level is remarkably low when computed on HF geometries optimized either in solution or in vacuo.

Since the solvent is described at the HF level even when an MP2 calculation in solution is performed [54],

Table 3. Solvent (THF) effect, G_{sol}, in kcal/mol, including non-electrostatic terms, on the adducts along the O···B approach path (Å) with the 6–31G* basis set

O···B	HF	MP2//HF_{vac}	MP2//HF_{sol}	MP2//$MP2_{vac}$	B3LYP
1.4	−5.92	−2.13	−2.35	−4.54	−4.76
1.5	−5.58	−1.73	−2.03	−4.32	−4.73
1.6	−5.36	−1.37	−1.87	−4.23	−4.52
1.7	−4.99	−1.04	−1.49	−3.97	−4.30
1.8	−4.84	−0.67	−1.27	−3.75	−4.23
1.9	−4.63	−0.26	−1.02	−3.56	−4.02
2.0	-	−0.03	-	−3.50	-
2.1	−4.27	0.22	−0.43	−3.37	−3.71

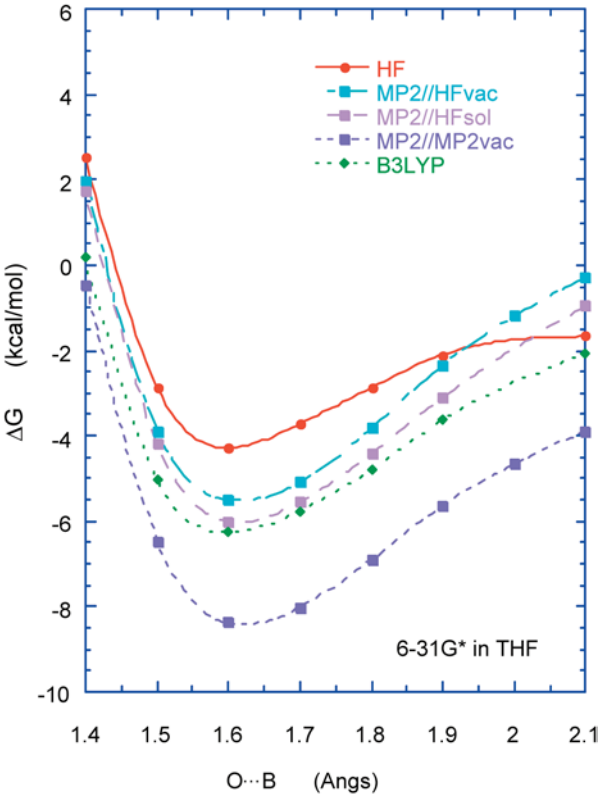

Fig. 15. HF and B3LYP/6–31G* interaction energy profiles with the inclusion of solvent effects in THF along the O···B approach path for complexes with acetone of oxazaboroline in the presence of a BH_3 at N, calculated at different levels on geometries optimised in THF solution. At the MP2 level three different geometries have been used (see text)

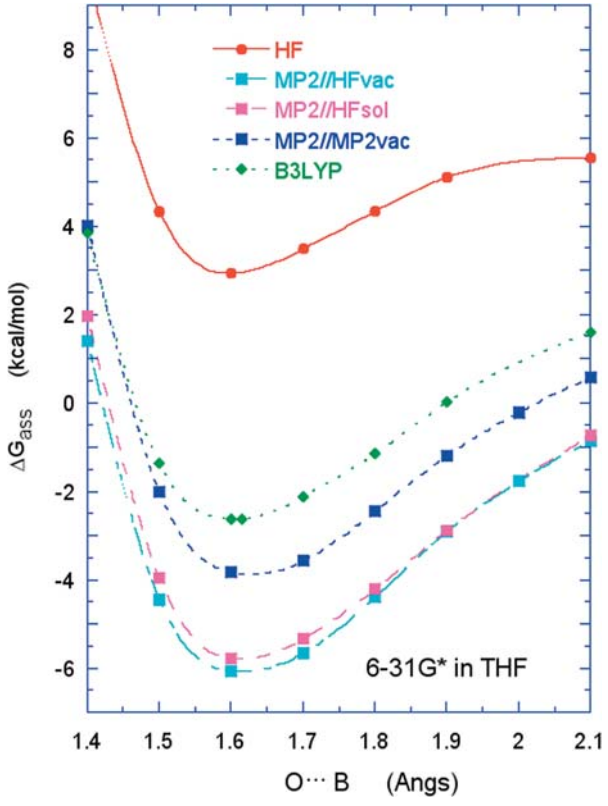

Fig. 16. HF and B3LYP/6–31G* association free energy profiles in THF along the O···B approach path for complexes with acetone of oxazaboroline in the presence of a BH_3 at N, calculated at different levels on geometries optimized in THF solution. At the MP2 level three different geometries have been used (see text)

the difference is clearly due to a considerable effect of the solute geometry, though they are fairly similar in the minimum as far as the intermolecular parameters are concerned (Electronic Supplementary Material, Tables S5–S6).

It is likely that correlation corrections somewhat affect the intramolecular structures. Nevertheless, the root mean square (rms) deviation between each couple of complex structures, computed at a B···O separation of 1.6 Å, is 0.10 Å for HF(vac) vs. MP2(vac), 0.08 Å for HF(vac) vs. HF(THF) and 0.14 Å for HF(THF) vs. MP2(vac). In all of the structures, one of the methyl groups of acetone is rotated by about 40° with respect to the minimum energy structure of isolated acetone (showing both methyl groups with the H *syn* with respect to the carbonyl O). In isolated acetone, this arrangement is higher in energy than the lowest energy structure by ∼0.3 kcal/mol at the B3LYP/6–31 + G** level. In the case of endo structures the rotated methyl group is the closest to the endocyclic O, as shown in Fig. 2, whereas in the case of exo structures the opposite occurs even though there is no steric hindrance or favorable interaction nearby.

A tentative evaluation of the association energy in THF solution, ΔG_{ass}, along the B···O approach path can be performed considering

$$\Delta G_{ass} = G_{SCF}(AB) - (G_{SCF}(A) + G_{SCF}(B)). \quad (14)$$

The curves, shown in Fig. 16, are closer to the corresponding ones obtained in vacuo (displayed in Fig. 3) than the curves relevant to the adduct solvation, shown in Fig. 15. The solvent effect (Eqs. 12 and 13), which is completely attributed to the complex in Fig. 15, is conversely reduced in Fig. 16 by the amount of solvent effect shown by the isolated partners.

Of course, the amount of G_{sol} for each isolated molecule should become lower as the other approaches, because partial desolvation occurs in the region where the molecules face each other. However, the real situation should correspond to intermediate values between these two boundaries. The HF/6–31G* free energies of association in THF are less favorable than the HF/6–31G* association energies obtained in vacuo. Conversely the B3LYP/6–31G* association values in solution are slightly more favorable than the association energies in vacuo. At the MP2/6–31G* level, the situation is reversed with respect to Fig. 15; the MP2(vac)/6–31G* structures, which are the best solvated adducts of Fig. 15, have a free energy of association in THF slightly worse than the association energy in vacuo, whereas the HF/6–31G* geometries (either obtained in vacuo or in solution) show the best association free energies in solution.

Conclusions

The trend of the association energies or free energies for the adducts between acetone and a model of the CBS catalyst along the B···O approach path is conserved regardless of the basis sets used, whether a variety of corrections are added or not. The corrections considered here (counterpoise corrections to BSSE, correlation corrections, thermal corrections in vacuo, solvent effects) actually affect the equilibrium energetic values, but not the shape of the curves, in that they consist in a shift of the energy scale. The prominent result is the existence of a local minimum in the region of the reactants in fair agreement with the experimental evidence [34]. To this end, the importance of the exocyclic BH_3 is clearly indicated by the monotonously decreasing trend of the energy curve along the B···O approach path obtained in its absence.

Counterpoise corrections, when computed with flexible geometries of the partners, should be deprived of deformation energy contributions in order to produce meaningful results.

Thermal corrections in vacuo sharply destabilize the complex, because of the loss of translational and rotational degrees of freedom of the isolated partners, whose entropic contribution is only recovered in part with vibrational contributions due to the new internal degrees of freedom of the complex.

The solvent (THF) effect obtained by solvating the already formed adduct is considerably more favorable than the association free energy in solution. The estimate of the latter should however take into account partial desolvation effects. Anyway, the real value should be located in-between these two limiting contributions.

Among the combination of basis sets and methods employed in this study, the B3LYP/6–31G* level is apparently the best suited to investigate the real system at a reasonable computational cost. If the 6–31G* (or more extended) basis set is used, even the HF results can be acceptable and, when CP corrected, they turn out to be comparable with the B3LYP and MP2 ones. MP2 results are actually too expensive, although, with reference to single point calculations performed on the HF/6–31G* geometries, they are the best approximation to the QCISD(T) curve.

From these considerations, B3LYP seems to be the method of choice, because, while giving a distinctly better description than HF, its computational cost is comparable to it and much lower than that of MP2, especially when geometry optimizations are to be performed.

Acknowledgements This work is dedicated to Jacopo Tomasi, to whom the authors are bound, though each at a very peculiar degree, by a long-lasting and strong personal and professional relationship. S.T. is grateful to DCCI for the award of a PhD studentship.

References

1. Ohno H, Hamaguchi H, Tanaka T (2001) Org Lett 3:2269
2. Ohno H, Ando K, Hamaguchi H, Takeoka Y, Tanaka T (2002) J Am Chem Soc 124:15255
3. Itsuno S, Nakano M, Miyazaki K, Masuda H, Ito K, Hirao A, Nakahama S (1985) J Chem Soc Perkin T 1:2039
4. Corey EJ, Bakshi RK, Shibata S (1987) J Am Chem Soc 109:5551
5. Umeyama H, Morokuma K (1976) J Am Chem Soc 98:7208
6. LePage TJ, Wiberg KB (1988) J Am Chem Soc 110:6642
7. Jonas V, Frenking G, Reetz MT (1994) J Am Chem Soc 116:8741
8. Anane H, Boutalib A, Tomás F (1997) J Phys Chem A 101:7879
9. Anane H, Boutalib A, Nebot-Gil I, Tomás F (1999) J Mol Struc–Theochem 463:53
10. Schwenke DW, Truhlar DG (1985) J Chem Phys 82:2418
11. Hawkins GD, Giesen DJ, Lynch GC, Chambers CC, Rossi I, Storer JW, Li J, Zhu T, Rinaldi D, Liotard DA, Cramer CJ, Truhlar DG (1998) AMSOL – Version 653. Regents of the University of Minnesota, MN
12. Møller C, Plesset MS (1934) Phys Rev 46:618
13. Pople JA, Binkley JS, Seeger R (1976) Int J Quantum Chem 10:1
14. Krishnan R, Frisch MJ, Pople JA (1980) J Chem Phys 72:4244
15. Frisch MJ, Trucks GW, Schlegel HB, Scuseria GE, Robb MA, Cheeseman JR, Zakrzewski VG, Montgomery Jr JA, Stratmann RE, Burant JC, Dapprich S, Millam JM, Daniels AD, Kudin KN, Strain MC, Farkas O, Tomasi J, Barone V, Cossi M, Cammi R, Mennucci B, Pomelli C, Adamo C, Clifford S, Ochterski J, Petersson GA, Ayala PY, Cui Q, Morokuma K, Malick DK, Rabuck AD, Raghavachari K, Foresman JB, Cioslowski J, Ortiz JV, Stefanov BB, Liu G, Liashenko A, Piskorz P, Komaromi I, Gomperts R, Martin RL, Fox DJ, Keith T, Al-Laham MA, Peng CY, Nanayakkara A, Gonzalez C, Challacombe M, Gill PMW, Johnson BG, Chen W, Wong MW, Andres JL, Head-Gordon M, Replogle ES, Pople JA (1998) Gaussian 98 (Revision,7). Gaussian Inc, Pittsburgh, PA
16. Becke AD (1993) J Chem Phys 98:5648

17. Lee C, Yang W, Parr RG (1988) Phys Rev B 37:785
18. Adamo C, Barone V (1998) J Chem Phys 108:664
19. Binkley JS, Pople JA, Hehre WJ (1980) J Am Chem Soc 102:939
20. Ditchfield R, Hehre WJ, Pople JA (1971) J Chem Phys 54:724
21. Hehre WJ, Ditchfield R, Pople JA (1972) J Chem Phys 56:2257
22. Dill JD, Pople JA (1975) J Chem Phys 62:2921
23. Hariharan PC, Pople JA (1973) Theor Chim Acta 28:213
24. Clark T, Chandrasekhar J, Spitznagel GW, von R Schleyer P (1983) J Comput Chem 4:294
25. Pople JA, Head-Gordon M, Raghavachari K (1987) J Chem Phys 87:5968
26. Miertus S, Scrocco E, Tomasi J (1981) Chem Phys 55:117
27. Tomasi J, Alagona G, Bonaccorsi R, Ghio C (1987) In: Maksic Z (ed) Modelling of structures and properties of molecules. Horwood, Chichester, p 330
28. Tomasi J, Persico M (1994) Chem Rev 94:2027
29. Barone V, Cossi M, Tomasi J (1997) J Chem Phys 107:3210
30. Tomasi S (2002) Applications for oxazaborolidine-catalysed reductions: a theoretical and experimental study of the double diasteroselective reduction of protected α-oximino-β-keto esters. PhD Thesis, Pisa University, Pisa, Italy
31. Alagona G, Ghio C, Persico M, Tomasi S (2003) J Am Chem Soc 125:10027
32. Nevalainen V (1991) Tetrahedron–Asymmetr 2:63
33. Linney LP, Self CR, Williams IH (1994) J Chem Soc Chem Comm 1651
34. Corey EJ, Link OJ, Bakshi RK (1992) Tetrahedron Lett 33:7107
35. Corey EJ, Helal PJ (1998) Angew Chem Int Edit 37:1986
36. Boys SF, Bernardi F (1970) Mol Phys 19:553
37. Jansen HB, Ros P (1969) Chem Phys Letters 3:140
38. Nagy PI, Smith DA, Alagona G, Ghio C (1994) J Phys Chem 98:486
39. Sokalski WA, Roszak S, Hariharan PC, Kaufman J (1983) Int J Quantum Chem 23:847
40. Alagona G, Ghio C, Monti S (2001) Int J Quantum Chem 83:128
41. Xantheas SS (1996) J Chem Phys 104:8821 (and refs quoted therein (9–13))
42. Rayón VM, Sordo JA (1998) Theor Chem Acc 99:68
43. Alagona G, Ghio C, Cammi R, Tomasi J (1987) Int J Quantum Chem 32:207
44. Thorne LR, Suenram RD, Lovas FJ (1983) J Chem Phys 78:167
45. Haaland A (1989) Angew Chem Int Edit 28:992 (and refs cited therein)
46. Alagona G, Ghio C, Monti S (2002) Int J Quantum Chem 88:133
47. In a discussion about the incidence of hindered rotations in the gas phase and in aqueous solution in the case of protonated norepinephrine [48], we concluded that only a very small fraction of molecules have the thermal activation energy needed to surmount the barrier
48. Nagy PI, Alagona G, Ghio C, Takács-Novák K (2003) J Am Chem Soc 125:2770
49. Alagona G, Ghio C, Nagy PI (submitted)
50. Wong MW (1996) Chem Phys Lett 256:391
51. Pople JA, Scott AP, Wong MW, Radom L (1993) Israel J Chem 33:345
52. Tidor B, Karplus M (1994) J Mol Biol 238:405
53. Alagona G, Germano G, Ghio C (2000) Theor Chem Acc 104:210
54. Olivares del Valle F, Tomasi J (1991) J Chem Phys 150:139